Procedia Manufacturing

Volume 1, 2015, Pages 327–342

43rd Proceedings of the North American Manufacturing Research Institution of SME http://www.sme.org/namrc

The Verification of the Mechanical Properties of Binder Jetting Manufactured Parts by Instrumented Indentation Testing

Yuhaowei Zhou[1], Yunlong Tang[1], Thibault Hoff[1], Martin Garon[2] and Fiona Yaoyao Zhao[1]

[1]*McGill University, Montreal, Canada.*

[2] *Biomomentum Inc., Laval, Canada*

yuhaowei.zhou@mail.mcgill.ca, tang.yunlong@mail.mcgill.ca, thibault.hoff@mail.mcgill.ca, garon@biomomentum.com, yaoyao.zhao@mcgill.ca

Abstract

In order to figure out the mechanical properties of freeform bio-medical parts made by Additive Manufacturing (AM), Instrumented Indentation Testing (IIT) is introduced to measure the Young's modulus from the free surface of the parts. The research also conducted several other different methodologies alongside the IIT in measuring the effective Young's modulus as a comparison. A special designed testing machine Mach-1^{TM} is used conducting the IIT, 3-point bending and compression test. The traditional compression test on standard cylinder parts made from the same binder jetting machine are used as a benchmark of the test material. Three different unit structures with different relative densities are considered, the solid part, the part with 1.0 mm size of grid lattice and the part with 1.5 mm size of grid lattice. Compared with the benchmark results obtained from traditional testing machines and the 3-point bending, the IIT bears a 15% error measuring solid and lattice freeform samples. Through the primary results, the porosity of the material as well as the stylus size and the lattice size contribute largely to the error.

Keywords: Instrumented Indentation Testing, Additive Manufacturing, lattice structure, Young's modulus, stylus size

1 Introduction

Additive Manufacturing (AM) technology tends to be used in special and customized parts. The shapes of these parts are usually irregular and not suitable for general mechanical testing methods.

Peer-review under responsibility of the NAMRI Scientific Committee

doi:10.1016/j.promfg.2015.09.038

Plus in some occasion, the destructive and large scale tests are not applicable. For example, on the biomedical implanted joints, traditional compression test is not applicable since the parts are to be implanted in human bodies, destructive test may, to some extent, deteriorate the part's mechanical properties. Plus the special shape of the joints makes it hard for traditional mechanical testing, thus specially designed fixtures are needed. The Instrumented Indentation Testing (IIT) is a development from the traditional mechanical tests. It is well suited for measuring small and freeform samples. It was mainly used in hardness testing. Different from traditional hardness testing, IIT conducts several measurements on one sample. Force and penetration are measured throughout the indenter's contact with the material (Hay 2009). The continuous measurements of force and displacement equip the IIT with a better tractability and higher accuracy. IIT can also be used in the measurement of Young's modulus from the force-displacement curve it obtained. These advantages enable the IIT to be a much more suitable mechanical testing method for biomedical use and parts fabricated via AM technology since the samples are mostly in freeform with complex structures. Currently, there is a promising trend of fabricating the bio-implant parts with AM technologies. A lot of researches are being conducted on 3D printed tissue scaffold, knees and hip replacement(Podshivalov et al. 2013).The flexibility and customization of AM satisfy the priority demanding of shaping. However, in term of quality and mechanical property, IIT provides an effective way in verifying these 3D printed parts. The paper will firstly introduce the IIT methodology in mechanical testing and then present the experiments conducted by Mach-1^{TM} mechanical tester on Additive Manufactured parts. The verification contains comparing the results of IIT with other traditional mechanical testing methods. The conclusion and analysis will be drawn at the end.

2 Methodology of Measurement

2.1 Instrumentation of IIT

The IIT system uses a specially designed probe tip to press against the surface of the sample, leaving the indent and at the same time measuring the force applied and the displacement. The generalization of the testing system is shown in Figure 1. Force is often applied using either electromagnetic or electrostatic actuation, and a capacitive sensor is typically used to measure displacement(VanLandingham 2003).

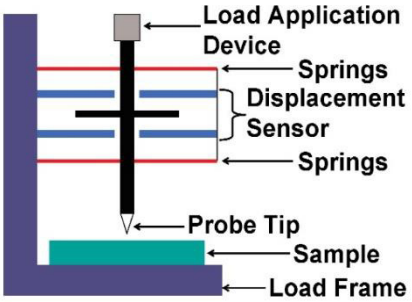

Figure 1: Schematic Illustration of an IIT system (VanLandingham 2003)

The forces and displacements start to be recorded continuously when the indenter first contacted the test surface. The force applied increases as well as the displacement until the pre-defined force or displacement is achieved. Then as the force decreases, the displacement generally recovers. The unloading curve will also be recorded. An indent may be left on the surface. Several of this iteration may apply to reduce the error of measurement.

2.2 Analysis and Calculation of IIT

Once the indentation test is done, the loading and unloading curves are obtained. The example of a typical curve is shown in Figure 2. During the IIT, as the indenter is driven into the material, both elastic and plastic deformation process occur and as the indenter is withdrawn, only the elastic portion of the displacement is recovered, which allows one to separate the elastic properties of the material from the plastic ones. The important quantities are the peak load (P_{max}), the maximum depth (h_{max}), the final depth after unloading (h_f) and the slope of the upper portion of the unloading curve (S) as shown in Figure 2.

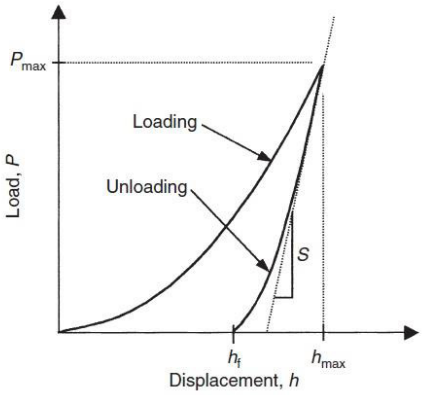

Figure 2: Indentation force-displacement curve (Hay and Pharr 2000)

The four quantities are directly measurable on the graph. To get the effective Young's modulus of the sample, the calculations shown in Equation (1) should be performed successively(Hay and Pharr 2000).

$$h_c = h_{max} - 0.75\frac{P_{max}}{S}$$

$$A = \pi h_c(D - h_c)$$

$$E_r = \frac{\sqrt{\pi}}{2\beta}\frac{S}{\sqrt{A}}$$

$$E = (1 - v^2)\left[\frac{1}{E_r} - \frac{1 - v_i^2}{E_i}\right]^{-1} \quad (1)$$

The variables in Equations are explained in the Nomenclature. The projected contact area formula A is based on the assumption that the indenter has no deviations from its perfect geometric shape; this formula is called the ideal area function(Hay and Pharr 2000).The Poison ratio v can be hard to determine, but even a rough estimate of ± 0.1 produces only about a 5% uncertainty in the calculated value of E for most materials. The geometry measurement of IIT is shown in Figure 3.

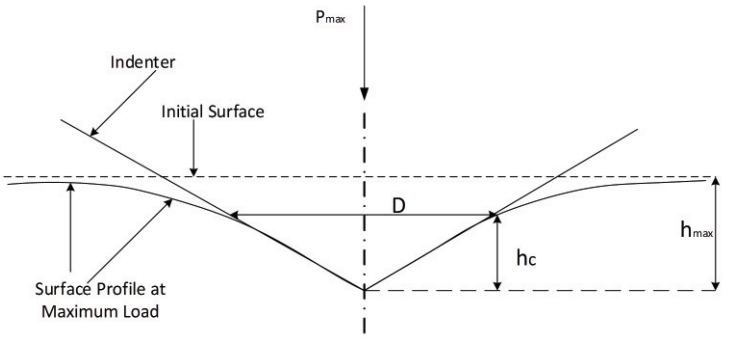

Figure 3: The IIT measurement schema

There are two very important criteria that must be satisfied in order to properly execute an IIT:

1. The equations hold true if and only if there is no pile-up during indentation. Pile-up is the phenomenon that happens together with plastic deformation. It may happen to certain material when sharp indenters or spherical indenters with large load are employed. The material around the contact impression plastically uplifts as shown in Figure 4. Pile-up cause a larger contact area than normal elastic contact. And the Hardness and Young's modulus will be overestimated due to contact area enlargement(Bolshakov and Pharr 1998). To reduce the possibility of pile-up phenomenon, the avoidance of using small stylus and rapid loading speed will help.

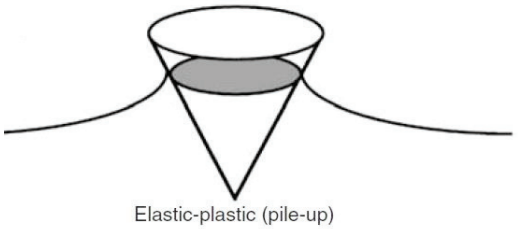

Figure 4: Phenomenon of pile-up during indentation

2. The surfaces of the tested samples should have a roughness much smaller than the contact diameter or the probe diameter. Since IIT are calculated from the contact depth and the area function based on the assumption that the measured surface is flat. Thus, the surface roughness is closely depend on the magnitude of the displacements and the contact area. To reduce the error that may be caused by the similar contact diameter and the magnitude of the surface roughness, either increasing the diameter of the probe or reducing the surface roughness should be applied.

3 Experiment Design and Testing

Currently available bone implants have limited flexibility on geometries. However, AM technology can produce freeform geometries of bone implants with much more complex than those produced using current conventional manufacturing technologies. The purpose of this research is to verify the reliability of IIT on Additive Manufactured parts in bone implant use. To achieve a better strength, metallic parts are always used in joints and bone replacement. Hollow and cellular designs

are always applied in order to lighten the weight and retain the space for organism to grow such as vessels and cartilage tissues. Binder Jetting AM technology satisfies the requirements for bone implant with a higher production flexibility and efficiency. Bio-compatible metallic materials can be employed with complex design. Higher manufacturing accuracy can be achieved with nano-level powder particles and fine nozzles. The verification research of IIT are based on Binder Jetting Additive Manufactured samples with both solid and cellular design. A specialized testing machine Mach-1™ (Biomomentum 2014) as well as a regular compression testing machine are used to carry out the tests. Alongside the benchmark traditional compression test, the 3-point bending tests are also employed to ensure the accuracy of the verification.

3.1 Testing Machine

Mach-1™ is a specially designed testing machine for bio-medical purpose. The multiple-axis tester can conduct various mechanical testing in a subtle manner that conforms to the bio-medical requirements. The testing machine is shown in Figure 4. There are various chambers used to perform compression, tension, indentation and bending tests on a universal displacement stage platform. The tests are mainly conducted in the vertical direction, the Z-axis. The following are some key factors of the Z-axis:

- the displacement resolution reaches100 nanometers with a travel range of 250 mm;
- the load goes up to ± 3.5 kg with a resolution of 175 mg;
- the acquisition rate of the stage position and the load cell signals goes up to 2.5 kHz which general 10 MB/min. of data;
- the maximum velocity goes for 50 mm/s with a maximum acceleration of 500 mm/s^2;
- load cell calibration and offset is available in the measurement

A camera with a macro lens is also set up to acquire high resolution images of 1280x960 on the part deformation. On the software side, the maximum displacement and the load cell speed is set. A finding contact program is employed to locate the surface of the sample before the application of the loading. The curve of load-displacement is generated accordingly as the test goes.

Figure 5: Mach-1™ testing machine and IIT stylus

3.2 Testing Part Design and Manufacturing

Both solid and cellular lattice structures are considered in the research to represent parts with different topologies and relative densities that conform to bio implant requirements. The lightweight lattice structure is a perspective direction in bone implant. Binder jetting AM technology performs very well in printing different lattice structures.

Besides the solid samples, the grid lattice structure of 1 mm and 1.5 mm are tested. The grid lattice is the basic form of homogeneous rigid lattice structure. It is easy to be generated from the CAD model of the design. The manufacturability of grid lattice is also high. Therefore, part consolidation and quality are assured. Figure 6 shows the samples of the three different part structures. For the grid lattice, the thickness of the lattice structure is 0.5 mm. The 1.0 mm size lattice has the space of 0.5 mm between the lattice struts and the 1.5 mm size lattice has 1.0 mm space between the struts as shown in Figure 6.

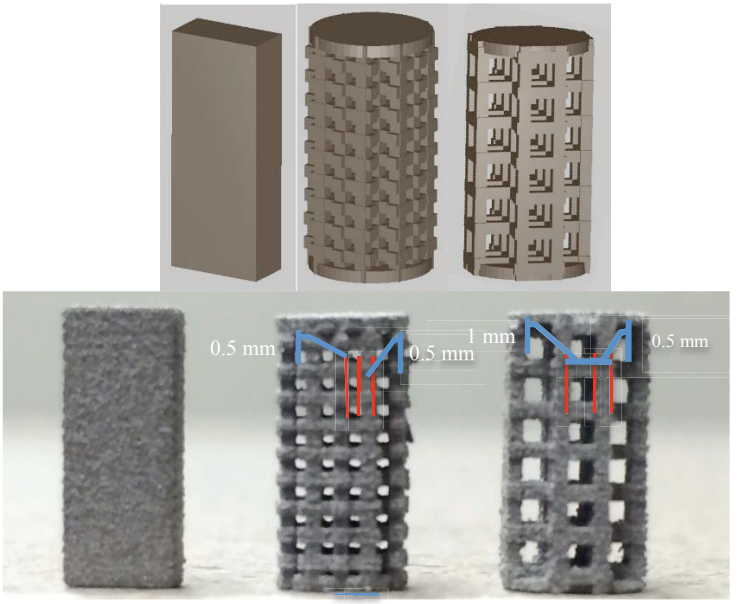

Figure 6: Different part structures: solid, grid lattice of 1.0 mm, grid lattice of 1.5 mm

The relative density plays an important role in the mechanical properties and it is also the key material factor in bio implant. The relative density of the lattice structure are calculated regarding the lattice struts as a type of homogenous material. The air in-between the struts also contribute to the volume of the parts. The relative densities of different lattice structures are calculated listed in Table 1.

Due to the working mode and material property of ExOne M-lab Binder Jetting manufacturing system, the solid part can achieve 52.4% dense for 30 μm particle size with regular one-step sintering program without any infiltration. The theoretical relative densities of the lattice structures then can be calculated according to the lattice size. In our experiments, the measured relative density has little difference of the theoretical ones.

	SSL-316 Powder	Printed solid parts	1.0 mm lattice	1.5 mm lattice
Theoretical Relative Density (g/cm^3)	8	4.19	2.1	1.1
Measured Relative Density (g/cm^3)	N/A	~4.1	~2.1	~1.0

Table 1: Relative densities of different part structures

Since the parts manufactured cannot achieve 100% dense, the parts are regarded as bulk isotropic cellular material. The geometric properties of the parts are not concerned in the research. All the mechanical properties mentioned in the research are refer as the effective properties of isotropic materials.

In order to conduct freeform testing, hemispheric parts in both solid and lattice structure are designed. These parts permit the IIT tests to be conducted from various angles and always easy to have a perpendicular testing surface to the probe. Although in measuring homogenous material, the perpendicularity of the probe is not required, it is extremely important when measuring the lattice structure which is not really homogenous in each direction. The sample parts are shown in Figure 7.

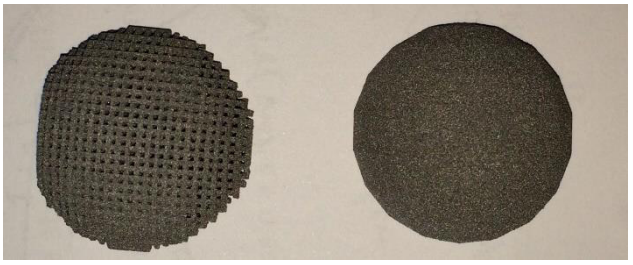

Figure 7: The hemispheric samples of 1.0 mm lattice and solid

All the testing parts are made from the powder of Stainless Steel -316 of 30 μm particle size. ExOne M-Lab (ExOne 2013) Binder Jetting Printer is used to manufacture the testing parts. The binder is a mixture of 75%-90% Ethylene Glycol Monomethyl Ether and 0%-15% Diethylene Gycol. The printer nozzle has a 30 μm resolution and works with a 70% binder saturation. The binder drying time is 30 s with a heating power of 75%. The green part is cured under 175 °C for 5 h and cooled down naturally before sintering. The sintering process firstly goes up to 630 °C holding 1.5 h and then reaches 1120 °C holding for another 1.5 h. No infiltration is involved in producing the testing part manufacturing.

3.3 Benchmark and Comparative Tests

In order to calibrate the testing machine and verify the IIT testing results in effective Young's modulus, traditional testing methods are also conducted. Since the Binder Jetting technology cannot produce a 100% dense part, plus the connections between the powder particles are isolate neck-connection, shown in Figure 8, the mechanical properties of the Binder Jetting printed parts are largely different from the standard Stainless Steel 316. In this case, a benchmark testing is needed to clarify the Young's modulus of the printed parts. Traditional compression tests on standard testing machine and with standard testing parts(ASTM E9-09 2010) are performed to generate the benchmark of the Young's modulus of the Binder Jetting printed Stainless Steel-316 parts.

For calibration purpose, the compression tests are also conducted on Mach-1^{TM} testing machine. However, due to the dimensional limitation of Mach-1^{TM}, the ASTM standard compression testing parts cannot physically fit. Smaller compression testing cylinders with different structures are manufactured. As a supplement to the compression tests, 3-point bending tests are also introduced to Mach-1^{TM} testing machine. With specially designed fixture, Mach-1^{TM} is able to conduct standard 3-point bending test.

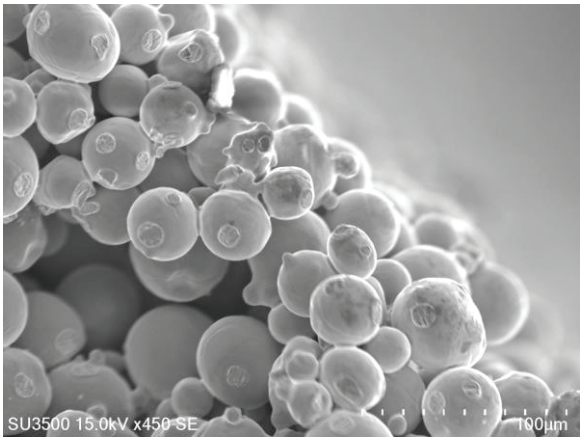

Figure 8: SEM of the test sample made by Binder Jetting AM

3.3.1. Traditional Compression Tests

BOSE 3510(BOSE 2014) Mechanical tester is used to conduct the standard compression test on the Binder Jetting printed standard cylinders. Short cylinder specimens of 13 mm diameter and 25 mm length are printed to obtain benchmark results(ASTM E9-09 2010). Five samples of each structure are tested with a loading speed of 0.01 mm/s to obtain a more accurate result.

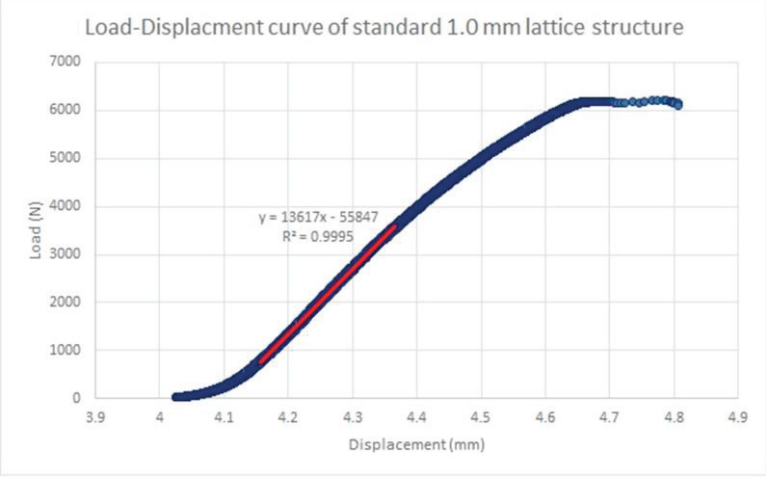

Figure 9: The load-displacement curve of a 1.0 mm standard cylinder specimen obtained from standard compression test

The load-displacement data is recorded for each specimens and the curve is generated as the example shown in Figure 9. The loading speeding is Linearly fitting is applied to obtain the slope of the linear section of the load-displacement curve. The slope represents the stiffness of the sample, which is 13617 N/mm. The Young's modulus is calculated from Equation (2). $F/\Delta L$ is the stiffness of the sample and can be represented by the slope rate of the load-displacement curve.

$$\mathrm{E} = \frac{\sigma}{\varepsilon} = \frac{F/A_0}{\Delta L/L_0} = \frac{FL_0}{A_0 \Delta L} \tag{2}$$

The standard test sample is designed to be 25 mm in length and 13 mm in diameter. However due to the possible manufacturing error, physical dimension measurements are conducted on each testing sample. 5 samples of each structural topology have been measured. The results are shown in Table 2. Since the stiffness is related to the structure besides the material, it is not within the scope of this study. The Young's modulus of each sample is calculated by Equation (2) and the average Young's modulus of each type of structure is the arithmetic mean of the five samples. The testing results are quite consistent of each structure. Thus, it is assumed that the benchmark of the Young's modulus of Binder Jetting manufactured samples are the average value of each type of structure.

Structural Topology	Average Length (mm)	Average Diameter (mm)	Average Young's modulus (GPa)
Solid Standard testing cylinder	25.00±0.33	13.00±0.19	4.07±0.29
Standard testing cylinder of 1.0 mm lattice structure	25.50±0.44	12.60±0.19	1.5±0.11
Standard testing cylinder of 1.5 mm lattice structure	24.70±0.35	12.50±0.09	0.446±0.08

Table 2: Standard compression testing results -- Benchmark

3.3.2. Mach-1^{TM} Compression Tests

The compression test of Mach-1^{TM} testing machine bears the same measuring principle of the standard testing machine. The displacement and the velocity are set before the test. The data of the displacement and load are recorded simultaneously as the load-displacement curve.

The compression tests on Mach-1^{TM} are using similar cylinders with smaller dimension as the standard compression test. Due to a smaller platform of Mach-1^{TM}, the test cylinders are re-scale to a smaller size. Avoiding buckling is the issue of compression test(ASTM E9-09 2010). To avoid buckling, the parts have a maximum length for a certain diameter. Though the exact Young's modulus is missing, estimation and calculation from the previous benchmark testing and the standard stainless steel shows that the maximum length and diameter ratio is extremely high. In this case, the design of test cylinder of 10.0 mm in length and 5.0 mm in diameter is validated for testing the mechanical property. This makes the result comparable to the benchmark testing. Three types of structural topologies are tested, the solid, the lattice of 1.0 mm and the lattice of 1.5 mm. Five samples of each types are tested to increase the results accuracy. The same as the BOSE 3510 traditional compression test, the loading speed of Mach-1^{TM} is also 0.01 mm/s. The Young's modulus is obtained the same as the standard compression test. The stiffness is represented by the slope of the load-displacement curve and the Young's modulus is calculated from Equation (2). 5 samples are measured in the tests. The results of the Mach-1^{TM} compression are shown in Table 3.

Structural Topology	Average Length (mm)	Average Diameter (mm)	Average Young's modulus (GPa)
Solid cylinder	9.90±0.05	4.98±0.03	3.95±0.12
Cylinder of 1.0 mm lattice structure	9.90±0.07	4.88±0.03	1.46±0.05
Cylinder of 1.5 mm lattice structure	10.03±0.03	5.04±0.11	0.41±0.04

Table 3: Mach-1 ^{TM} compression tests results

Compare to the benchmark testing, the Young's modulus obtained from Mach-1^{TM} compression tests bears a very little difference as shown in Table 4. From Table 2 and Table 3, it can be seen that for each type of structural topology, the Young's modulus obtained from the Mach-1^{TM} compression tests are about 3%-9% smaller than the one obtained from the standard compression test. This difference is allowable due to the different testing machine structure and manufacturing accuracy. The

difference can also be used as calibration of Mach-1™ testing machine and to compensate the IIT results in the verification.

Structural Topology	Young's Modulus-STD (GPa)	Young's Modulus-Mach-1 (GPa)	Difference (%)
Solid	4.07	3.95	**2.95**
1.0 mm lattice	1.50	1.46	**2.67**
1.5 mm lattice	0.446	0.407	**8.74**

Table 4: Compression tests results comparison

3.3.3. Mach-1™ 3-point Bending Test

Considering the flexural mechanical response of the sample, 3-point bending test is introduced to the IIT verification test. A specially designed fixture with loading and supporting rollers is used to adapt the 3-point bending test to Mach-1™ testing machine. The testing samples are, according to ISO 4049, rectangular bar-shaped specimens. As the rectangular bar-shaped specimen bends under loading, tensile stresses on the lower convex surface of the specimen are most likely responsible for initiating failure(Darvell 2009). The 3-point bending test has simpler stress field than in compression test and diameter tensile test(Darvell 1990). The Young's modulus of the specimen can be calculated from Equation (3). F/δ is the slope of the load-displacement curve. I is the second moment of inertia of the testing geometry, for rectangular bar, $I = \frac{bh^3}{12}$ where b is the width and h is the height of the testing sample.

$$E = \frac{FL^3}{48\delta I} \tag{3}$$

The rectangular bar-shape testing samples are designed to fit in the Mach-1™ machine. The dimension is 60x10x5 mm and the distance between the two supporting rollers are 38 mm. Five samples of each structural topology are tested and the results are shown in Table 5. In the calculation, the distance between the two support rollers are fixed and is exact 38 mm. However due to the manufacturing uncertainty, the part dimension is not 100% accurate. Physical measurements of height and width are applied before testing.

The results shown in Table 5 indicate that 3-point bending test of Mach-1™ has achieved a deviation of less than 10% with both the standard compression test and Mach-1™ compression test. This difference may be caused by the testing error or the manufacturing error of the samples.

From the results of compression test and 3-point bending test, Mach-1™ can be considered as an accurate mechanical testing machine. Base on this condition, the IIT verification can be achieved.

Structural Topology	Average Height (mm)	Average Width (mm)	Average Young's modulus (GPa)
Solid rectangular bar	5.13±0.02	10.00±0.07	4.40±0.32
Rectangular bar of 1.0 mm lattice structure	5.05±0.05	10.01±0.06	1.41±0.08
Rectangular bar of 1.5 mm lattice structure	4.95±0.05	9.92±0.07	0.46±0.04

Table 5: Mach-1 ^{TM} 3-point bending tests results

3.4 IIT Verification

The advantage of IIT is the measuring flexibility on freeform surface. However, the indentation stylus has to be perpendicular to the measuring surface in measuring the heterogeneous material, in this case, the lattice structure. In the verification process, IIT are conducted on hemispheric samples from different angles. To assure the perpendicularity, the samples are designed to have the hemispheric surface generating from small square surfaces as shown in Figure 10. These square surfaces helps to easily adjust the stylus to be perpendicular to the measuring surface in different angles.

The IIT are conducted in three different points of each sample: one point on the top position parallel to the platform, two on each side with 30° incline to X-axis as shown in Figure 11. The

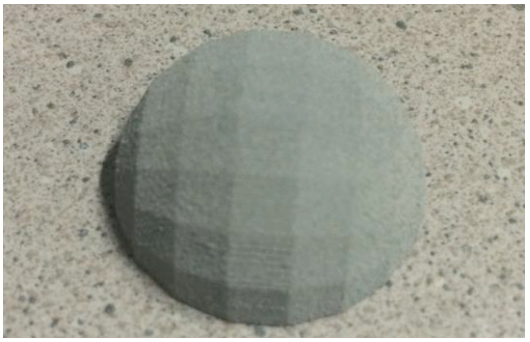

Figure 10：The surface of the hemispheric sample

samples are fixed on the platform which can be tilted. The indentation stylus is always in the vertical position. Three samples of each structural topology are measured. In total, nine samples are tested. Three times indentation on each sample at each angle are measured and the arithmetic mean of the Young's modulus is calculated.

The smaller the stylus size is the more flexible the measurement could be. However, in measuring the lattice structure, at micro level, the structure is not isotropic. If the lattice structure is treated as a homogenous material, the measurements should avoid similar dimensional stylus as the lattice size. Larger size of indentation stylus are preferred. In this case, two different indentation stylus are used in the experiments, the stylus of 6.0 mm diameter and the stylus of 1.0 mm diameter. For each solid sample, both indentation stylus are used in the measurement. For lattice sample, only the smaller stylus is used in measurements. 108 measurements are conducted.

Figure 11: The IIT measurements on spherical parts

During the IIT, it is assumed that no pile-up phenomenon happens. 3 ramps are performed in each test. And the releasing condition is 0.05 mm depth from the contact surface. The Young's modulus is calculated according to Equation (1). The effective Poisson ratio of the printed steel powder can be obtained from the theory reported by Arnold, Boccaccini, and Ondracek (1996). The stainless steel has the original Poisson ratio of 0.27 and the effective Poisson ratio of 50% porous stainless steel is 0.172. According to Equation (1), the Poisson ratio will not significantly affect the final Young's modulus. Hence, Poisson ratio of 0.172 is taken as the inherent Poisson ratio of the Binder Jetting printed stainless steel parts(Arnold, Boccaccini, and Ondracek 1996). For the lattice structure, according to Arnold, Boccaccini, and Ondracek (1996), the porous density and its effect on Poisson ratio, the effective Poisson ratio of 1.0 mm lattice and 1.5 mm lattice can be obtained from their relative density towards the solid parts. The results are shown in Table 6. The stylus of the Mach-1^{TM} machine is made of Stainless Steel AISI 316L with a Poisson ratio of 0.30 and Young's modulus of 200 GPa (as the v_i and E_i in Equation (1)).

In the calculation using Equation (1), the S is the slope of the unloading curve. h_{max} is the maximum displacement of the contact point. P_{max} is the maximum load applied. All of the three parameters can be acquired from the Load-displacement curve as the example shown in Figure 12. The experiments results are shown in Table 7.

	Relative Density	Poisson Ratio	Young's Modulus (GPa)
Stainless Steel	100%	0.27	200
Binder Jetting Printed Stainless Steel	~50%	0.172	4.07
Binder Jetting Printed 1.0 mm lattice Stainless Steel	~25%	0.127	1.50
Binder Jetting Printed 1.5 mm lattice Stainless Steel	~12.5%	0.107	0.446
Mach-1 tester Stylus	N/A	0.30	200

Table 6: Poisson ratio and Young's modulus using for IIT test

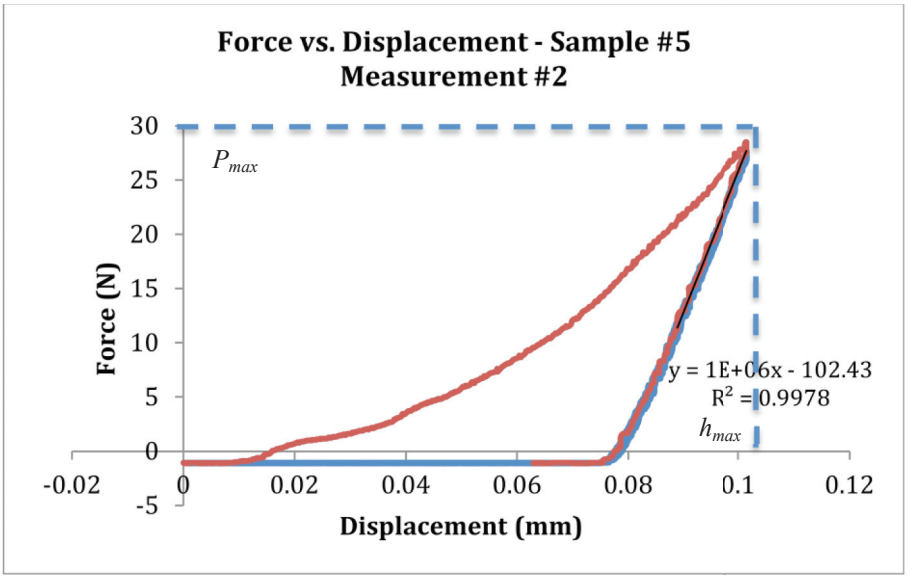

Figure 12 : IIT load-displacement curve for Young's modulus and stiffness calculation

4 Result and Analysis

From the results in Table 7, the Young's modulus measured by IIT is smaller than the benchmark and the results obtained from Mach-1™ compression test on the solid samples and 1.0 mm lattice samples. The error ranges from 13% to 54%. On the 1.5 mm lattice sample, the IIT results turn out to be larger than the benchmark, almost reaching 1.5 times the benchmark value. For each sample, either solid or with lattice structure, the measurement at horizontal position is larger than the measurements with inclines. On the solid samples, the measurement with smaller indentation stylus has achieved more relevant result than the one with larger stylus. The smaller stylus bears 13% error compares to 46.3% error of the larger stylus at the horizontal position.

Equation (1) signifies the importance of unloading slope S in determining the Young's modulus of IIT testing results as explained in 2.2. Compared to the horizontal position, the incline position has a smaller result which may be caused by the smaller slope of the unloading load-displacement curve. The smaller slope indicates smaller plastic deformation on the sample during the indentation. This may be caused by the inhomogeneous material distribution of Binder Jetting technology plus the uncertainty in stylus's perpendicularity towards the measuring surface as mentioned in 3.2. The two factors together cause an unsteady indentation which leads to less plastic deformation of measuring surface.

Considering the larger indentation stylus, larger diameter brings a larger contact area A. It should also bring a steeper loading and unloading curve since with larger contact area, the same amount of load causes smaller deformation, refer to 2.2. However, because of the porosity of the Binder Jetting printed parts, the weakly connected powder particles may collapse at the beginning of the contact. This leads to a similar slope in the loading and unloading curve to the smaller stylus. In calculation with Equation (1), the larger contact area A then leads to a smaller Young's Modulus. With lattice structure, this kind of particle collapse may happens earlier than it should be when the relative density goes extremely low. This explains why the 1.5 mm lattice has larger testing results than the benchmark. A quicker particle collapse generates a steeper unloading curve. From Equation (1), the abnormally smaller S causes a larger reduced modulus E_r that leads to a larger Young's modulus.

Categories	Sample	Horizontal	30° Incline	30° Incline 2	Benchmark Young's modulus (GPa)
Solid – 1.0 mm indentation stylus	Sample 1	3.35	3.01	3.13	
	Sample 2	3.82	3.21	3.32	
	Sample 3	3.42	2.83	3.14	**4.07**
	Average	**3.53**		**3.11**	
	Error	**-13.05%**		**-23.40%**	
Solid -6.0 mm indentation stylus	Sample 1	2.33	1.78	1.82	
	Sample 2	1.98	1.86	1.85	
	Sample 3	2.24	1.89	1.84	**4.07**
	Average	**2.18**		**1.84**	
	Error	**-46.30%**		**-54.70%**	
Lattice of 1.0 mm	Sample 1	1.40	0.87	0.92	
	Sample 2	1.23	0.78	0.88	
	Sample 3	1.25	0.78	0.73	**1.50**
	Average	**1.29**		**0.83**	
	Error	**-14.00%**		**+44.70%**	
Lattice of 1.5 mm	Sample 1	0.64	0.49	0.48	
	Sample 2	0.67	0.59	0.49	
	Sample 3	0.69	0.46	0.50	**0.446**
	Average	**0.67**		**0.50**	
	Error	**+50.20%**		**+12.10%**	

Table 7: IIT result of hemispherical sample

The most reliable result achieved by IIT on Binder Jetting printed parts is the measurement of the solid spherical part at the horizontal position with an error of 13.05%. Although the measurement on 1.5 mm lattice at incline position has a smaller error of 12.1%, it may not be viewed as reliable due to the particle collapse descripted previously. On the 1.0 mm lattice structure, the 6 mm diameter stylus also achieved a 14% error when measuring at the horizontal position.

5 Conclusion and Future Work

IIT has long been used in hardness and elasticity testing for the purpose of material quality control (VanLandingham 2003) . The technique is mainly devoted in measuring isotropic material or parts made from conventional manufacturing. As the propagation of AM technology and the development of cellular material, more and more anisotropic material and parts come into use. The research has conducted several methods in verifying the IIT testing method in determining the Young's modulus of Binder Jetting additive manufactured parts. A specially designed mechanical tester Mach-1 is employed in conducting IIT. Through the experiments conducted on traditional mechanical testing machine, the research set up a benchmark Young's Modulus of the Binder Jetting additive manufactured sintered stainless steel parts. Due to the special manufacturing process of Binder Jetting Additive Manufacturing, the powder particles form a weak neck connection among each other which can only achieve a Young's Modulus of 4.07 GPa, far from the 200 GPa of a regular stainless steel. The Young's Modulus goes even less for the lattice structural parts. 1.50 GPa for 1.0 mm size grid lattice and 0.446 GPa for 1.5 mm size grid lattice. Compression tests and 3-point bending tests conducted on Mach-1^{TM} mechanical tester have obtained similar results as the benchmark which verifies the reliability of the tester.

The IIT are conducted on hemispherical parts which represents the freeform parts which IIT is designed for. The testing results shows about 15% error when measuring Young's modulus at horizontal position while a larger error happens when measuring at a inclined position. The angle between the stylus and measuring surface is critical in measuring non homogenous material.

The calculation of Young's modulus from the loading-unloading displacement curve will also need to be calibrated. An impact factor is recommended to apply according to different stylus size and the lattice size.

Further study will try to clarify the effect of the indentation angles towards the measuring surface during the IIT experiment as well as identifying the correlation factors between the lattice size and the indentation stylus during the measurements.

Acknowledgements

This research work is supported by Biomomentum Inc. and National Science and Engineering Research Council Engage Grant 462653-14.

Nomenclature

h_c	the contact depth, which for elastic contact is less than the total depth of penetration h_{max}
h_{max}	the maximum contact depth of indentation
D	the diameter of the indenter
A	the projected contact area of IIT
A_0	the original cross-sectional area through which the load is applied in 3-point bending test
E	the Young's modulus of the test material
E_r	the reduced modulus, accounting for the elastic displacements that occurs in both the indenter tip and the sample
E_i	Young's modulus of the indenter
F	the load applied on the sample in IIT
I	the second moment of inertia of the testing geometry in 3-point bending test
L	the distance between the two supporting roller in 3-point bending test
L_0	the original length of the sample
ΔL	the amount by which the length of the sample changes
S	the slope of the unloading curve of IIT
v	the Poisson's ratio for the test material
v_i	the Poisson's ratio of the indenter
β	according to Bulychev et al. (1975) is the constant that depends on the geometry of the indenter. In case of circular contacts, $\beta=1$(Hay and Pharr 2000)
σ	the compression stress
ε	the compressional strain
h	the height of the testing sample in 3-point bending test
b	the width of the testing sample in 3-point bending test
δ	the deformation happens in 3-point bending test

References

Arnold M, Boccaccini AR and Ondracek G. Prediction of the Poisson's ratio of porous materials. *Journal of Materials Science* 1996; 31 (6):1643-1646.

ASTM E9-09. Standard Test Methods of Compression Testing of Metallic Materials at Room Temperature. ASTM International 2010.

Biomomentum. Mechanical Testing System- Mach-1™. http://www.biomomentum.com/ 2014.

Bolshakov A and Pharr GM. Influences of pileup on the measurement of mechanical properties by load and depth sensing indentation techniques. *Journal of materials research* 1998;13 (04):1049-1058.

BOSE. Bose ElectroForce|3500 All-Electric Test Instruments. http://worldwide.bose.com/electroforce/en_us/web/3500_products/page.html 2014.

BulychevSI, Alekhin VP, Shorshorov MH, Ternovskii AP, and Shnyrev GD. Determining Young's modulus from the indentor penetration diagram. *Ind. Lab* 1976; 41 (9):1409-1412.

Darvell BW. *Materials science for dentistry*: Elsevier 2009.

Darvell BW. Uvniaxial compression tests and the validity of." *Journal of Materials Science* 1990; 25 (l990):757-780.

ExOne. X1-Lab. http://www.exone.com/en/materialization/systems/X1-Lab 2013.

Hay J. Introduction to instrumented indentation testing. *Experimental Techniques* 2009;33 (6):66-72.

Hay J. and Pharr GM. Instrumented Indentation Testing. *ASM Handbook* 2010; 8 (Mechanical Testing and Evaluation).

Podshivalov L, Cynthia MG , Andrea Z, Jens G, Pinhas BY and Anath F. Design, Analysis and Additive Manufacturing of Porous Structures for Biocompatible Micro-Scale Scaffolds. *Procedia CIRP* 2013;5(0):247-252. doi: http://dx.doi.org/10.1016/j.procir.2013.01.049.

VanLandingham MR. Review of instrumented indentation. *Journal of Research of the National Institute of Standards and Technology* 2003;108 (4):249-265.